

The effect of soil texture, layering and water head on the infiltration rate and infiltration model accuracy

Azizeh Alizadeh Berdouki¹ Cristina Cruz³

¹Department of Water Engineering, Faculty of Agriculture, Urmia University, Urmia, Iran

²Urmia Lake Research Institute, Urmia University, Urmia, Iran

³Centre for Ecology, Evolution, and Environmental Changes (cE3c) & CHANGE—Global Change and Sustainability Institute, Faculty of Sciences, University of Lisbon, Lisbon, Portugal

Correspondence

Sina Besharat, Department of Water Engineering, Faculty of Agriculture, Urmia University, Urmia, Iran. Email: s.besharat@urmia.ac.ir

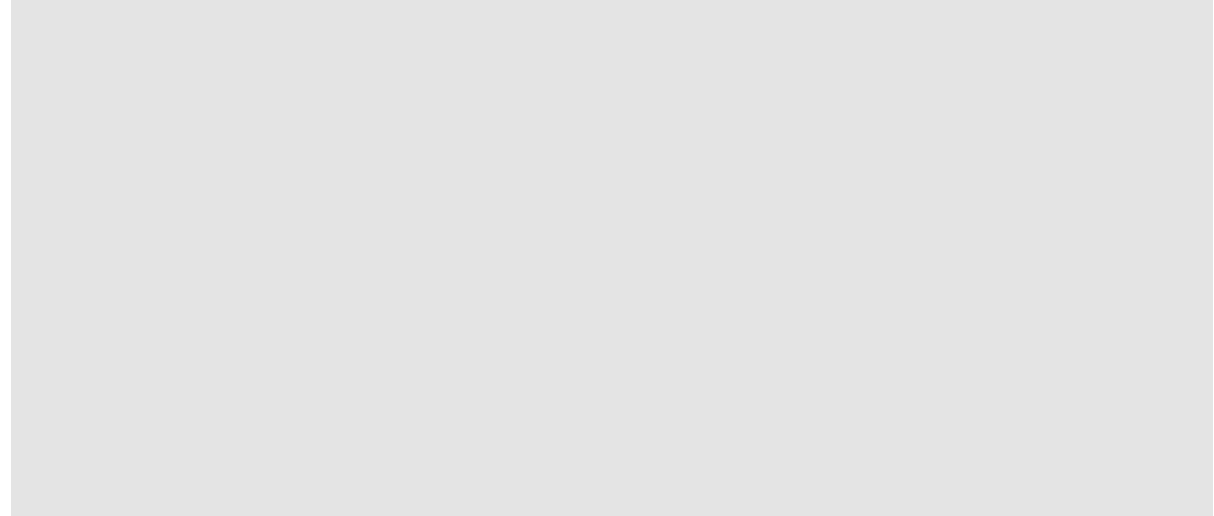
Funding information

Urmia University

Abstract

Infiltration is one of the most important physical characteristics of soil and depends on various factors. This study investigated the influence of soil texture, layering and water head on the soil water infiltration rate. It also selected the most accurate infiltration models to determine the water infiltration rate in homogeneous and heterogeneous soil profiles. Experiments were carried out in four soil containers with a length, width and height of 20 × 20 × 70 cm. Treatments consisted of two soil textures (sandy loam, SL; clay loam, CL), four soil profiles (homogeneous texture, SL and CL; and heterogeneous texture, lighter texture on the top, SL/CL, and heavier texture on the top CL/SL) and three water head sizes (4, 7 and 10 cm). Several models were used to determine the water infiltration rate under homogeneous (Kostiakov, modified Kostiakov, Philip, Horton, traditional Green–Ampt, modified Green–Ampt and HYDRUS-1D) and heterogeneous soils (traditional Green–Ampt, modified Green–Ampt and HYDRUS-1D). According to the results, the infiltration rate decreased over time and along the soil profile. Nevertheless, it jumped at the interface of two-layered soils when the heavier soil was in the bottom layer (SC treatments) due to the high potential of the second layer, and then it decreased. In the reverse layering, the infiltration rate in the interface was lowest (CS treatments) because of the higher hydraulic conductivity of the second layer. Additionally, the infiltration rate increased with increasing water head, but the rate of this increase was higher by changing the water head from 7 to 10 cm. The results of infiltration models showed that the accuracy of these models was higher in clay loam texture than in sandy loam texture. The modified Green–Ampt was the most accurate model in homogeneous and layered soils, with average RMSE of 0.0204 and 0.019, respectively. The Horton model had the weakest simulation in homogeneous soils, with

an average RMSE of 0.1299. Additionally, the accuracy of HYDRUS-1D in layered soils was less than that in homogeneous soils (NS of 0.95 and 0.85, respectively), and its accuracy decreased with increasing water head in most treatments.



Article title in French: L'effet de la texture du sol, de la superposition et de la chute d'eau sur le taux d'infiltration et la précision du modèle d'infiltration.

846 © 2024 John Wiley & Sons, Ltd. [wileyonlinelibrary.com/journal/ird](https://onlinelibrary.wiley.com/journal/ird) Irrig. and Drain. 2024;73:846–865.

BERDOUKI ET AL.

847

15310361, 2024, 3, Downloaded from

<https://onlinelibrary.wiley.com/doi/10.1002/ird.2918> by Faculdade Medicina De Lisboa, Wiley Online Library on [22/01/2025]. See the Terms and Conditions

(<https://onlinelibrary.wiley.com/terms-and-conditions>) on Wiley Online Library for rules of use; OA articles are governed by the applicable Creative Commons License



KEYWORDS

HYDRUS-1D model, infiltration models, layered soils, soil texture, water head

Résumé

L'infiltration est l'une des caractéristiques physiques les plus importantes du sol et dépend de divers facteurs. Cette étude a examiné l'influence de la texture du sol, de la superposition et de la charge d'eau sur le taux d'infiltration de l'eau dans le sol. Elle a

également sélectionné les modèles d'infiltration les plus précis pour déterminer le taux d'infiltration d'eau dans des profils de sol homogènes et hétérogènes. Les expériences ont été réalisées dans quatre contenants de terre d'une longueur, d'une largeur et d'une hauteur de 20 x 20 x 70 cm. Les traitements ont consisté en deux textures de sol (loam sableux—SL, loam argileux—CL), quatre profils de sol (texture homogène—SL et CL; et texture hétérogène, texture plus légère sur le dessus—SL/CL, et texture plus lourde sur le dessus CL/SL) et trois tailles de chute d'eau (4, 7 et 10 cm). Plusieurs modèles ont été utilisés pour déterminer le taux d'infiltration de l'eau sous des sols homogènes (Kostiakov, Kostiakov modifié, Philip, Horton, vert traditionnel ampt, vert modifié ampt et HYDRUS-1D) et hétérogènes (vert traditionnel ampt, vert modifié ampt et HYDRUS-1D). Selon les résultats, le taux d'infiltration a diminué au fil du temps et le long du profil du sol. Néanmoins, il a scellé à l'interface des sols à deux couches lorsque le sol plus lourd se trouvait dans la couche inférieure (traitements SC) en raison du potentiel élevé de la deuxième couche, puis il a diminué. Dans la couche inversée, le taux d'infiltration à l'interface était le plus faible (traitements au CS) en raison de la conductivité hydraulique plus élevée de la deuxième couche. De plus, le taux d'infiltration augmentait avec l'augmentation de la chute d'eau, mais le taux de cette augmentation était plus élevé en changeant la chute d'eau de 7 à 10 cm. Les résultats des modèles d'infiltration ont montré que la précision de ces modèles était plus élevée dans la texture argileuse que dans la texture sablonneuse. Le modèle vert modifié ampt était le plus précis pour les sols homogènes et stratifiés, avec des RMSE moyens de 0,0204 et 0,019, respectivement. Le modèle de Horton présentait la simulation la plus faible dans des sols homogènes, avec un RMSE moyen de 0,1299. De plus, la précision de l'HYDRUS-1D dans les sols stratifiés était inférieure à celle des sols homogènes (NS de 0,95 et 0,85, respectivement), et sa précision diminuait avec l'augmentation de la charge d'eau dans la plupart des traitements.

MOTS CLÉS

modèle HYDRUS-1D, modèles d'infiltration, sols stratifiés, texture du sol, chute d'eau

1 | INTRODUCTION

Water infiltration into the soil is a critical process in many aspects and is a great concern in many fields, such as hydrology, agriculture and geotechnical and geological engineering (Cheng et al., 2021). The effective design of the water resources system depends on the accuracy

of infiltration estimation since the volume of infiltration is the main input in the analysis design of the water resources system (Harisuseno & Cahya, 2020). Many models have been provided for infiltration prediction, often due to the importance of infiltration (Chari et al., 2020). Using infiltration models allows for irrigation optimization while reducing time and cost waste in

field infiltration measurements, especially at the catchment scale. Infiltration equations are divided into physical, empirical and semi-empirical equations. Empirical and semi-empirical equations, such as Kostiakov (1932), are simple models that are usually determined from empirical data (Mishra et al., 2003). However, these equations cannot describe the details of the infiltration process as well as physical models (Ma et al., 2010). The Green-Ampt and Richards equations have been the most common physical models (Ma et al., 2010). The HYDRUS-1D model, based on the Richards equation, is an advanced model for simulating water, heat and solute

movement in the soil and for predicting root water absorption and growth (Simunek et al., 2005).

The rate of water infiltration depends on the soil texture, soil structure, soil compaction, initial soil moisture, layering and depth of the soil profile, groundwater level, ground slope and soil surface conditions such as vegetation and water head (Al-Ghazal, 2002; Garg & Goel, 2019; Hillel, 1998). Patle et al. (2019) estimated the infiltration rate using a regression model based on soil characteristics at 25 points on cultivated land with a 10-m grid interval. Field measurements were performed using a double ring. The results showed that sand, particle density and organic carbon content have a positive correlation with infiltration rate, whereas silt, clay, bulk density and moisture content have a negative correlation with it. Additionally, the multilinear regression model was the best one for estimating infiltration. Modelling water consumption in soil under wheat–corn cultivation showed that water movement is closely related to the thickness and relative position of layers with distinct textures along the soil profile (He et al., 2013; Ma et al., 2016).

It has been agreed that water head influences water infiltration (Erie, 1962), and it is known that, for the same initial conditions (Al Shakerchy, 2009), the water infiltration rate increases with increasing water head size (Al-Ghazal, 2002). However, except for the Green–Ampt model, water head size is not directly involved in any other infiltration model, which may be the origin of the discrepancies observed between the empirical and estimated water infiltration rates.

The Kostiakov model (1932) is the oldest empirical water infiltration model and contemplates the influence of rainfall intensity, initial soil moisture, bulk density, texture and vegetation (Adindu et al., 2014; Parhi, 2014). It is simple (Clemmens, 1983) and widely used in surface irrigation (Furman et al., 2006). To be suitable for application in long-term determinations, it was modified by adding a constant coefficient equal to the final infiltration rate (Mezencev, 1948). The Horton model (Horton, 1940) is another valid empirical equation in hydrology that considers the final water infiltration rate as a function

corrected by a coefficient determined by texture and initial soil moisture.

The physical models used to calculate the water infiltration rate are based on physical laws and are consequently ideal under controlled experimental conditions but not good for describing water infiltration under actual soil conditions. Philip's model (Philip, 1957) describes water infiltration in vertical and horizontal directions based on soil sorptivity and initial and final moisture. It is a good model to predict the water infiltration rate for extended periods since, at the beginning of the infiltration process, soil sorptivity (a function of soil suction) is dominant (Adindu et al., 2015). The HYDRUS-1D model can predict the flow of water under different pore saturation conditions using the numerical solution of the one-dimensional Richards equation (Simunek et al., 2005) considering the volumetric moisture content of the soil, water head pressure and unsaturated soil hydraulic conductivity estimated by van Genuchten et al. (1991). The Green and Ampt (1911) equation was developed to calculate the water infiltration rate for homogeneous soils with constant water heads. However, this model is also used in heterogeneous soils. It is assumed that each soil layer is homogeneous, the interface between adjacent layers is sharp, and the initial moisture content in each layer is uniform (Mohammadzadeh-Habili & Heidarpour, 2015). This model considers the flow in the unsaturated zone influenced by soil suction and in the saturated zone influenced

by the gravity potential and constant suction head of the moisture front and expresses the infiltration rate in this zone according to Darcy's law (Green & Ampt, 1911). The Green–Ampt model was modified to incorporate the air entry to the soil column and estimate the actual hydraulic conductivity of the saturated area less than the saturated hydraulic conductivity (Ma et al., 2010).

Taking into consideration the distinct nature of the models most used to determine the soil water infiltration rate, it is expected that they point to distinct results when considering the interaction between texture heterogeneity along the soil profile and water head size, since most of the equations were optimized for specific values of each of these variables (Abdulkadir et al., 2011; Adindu et al., 2015; Ali et al., 2016; Dagadu & Nimbalkar, 2012; Furman et al., 2006; Haghghi et al., 2010; Hajabbasi, 2006; Liu et al., 2008; Ma et al., 2011; Mohammadzadeh-Habili & Heidarpour, 2015; Navar & Synnott, 2000; Oku & Aiyelari, 2011; Sihag et al., 2017; Šimušek et al., 2008).

Mohammadzadeh-Habili and Heidarpour (2015) conducted experiments in six columns of two-layered soil with different permeabilities and constant heads to evaluate the Green–Ampt model. The results showed that

when the first layer is more permeable, the infiltration rate at the two-layer interface increases significantly. However, when the first layer is less permeable, the infiltration velocity at the two-layer interface is lower than the final infiltration velocity in the lower layer.

In this study, the effect of water head on infiltration model accuracy was investigated, which has been addressed in only a few studies (Al Shakerchy, 2009; Al-Ghazal, 2002; Hsu et al., 2017). The main purpose of this research was to study the effect of water head, texture, layering and their interaction effect on infiltration rate. Additionally, this study investigated the interaction effect of texture, layering and water head on the infiltration rate in homogeneous and heterogeneous soils, which has not been discussed in other research.

2

|

MATERIALS AND METHODS Columns preparation

2.1

|

The experiments were conducted at the Hydraulic Laboratory of the Water Engineering Research Department of Urmia University, Iran, in 2017. Soil texture was assessed based on the hydrometer analysis test (Bouyoucos, 1962; Gee & Bauder, 1986), bulk density of soil layers was obtained from the core method (Ma et al., 2010), soil density was determined using the pycnometer (Soil Survey Staff, 2004), and saturation hydraulic conductivity was obtained using the constant head water method (Liu et al., 2008). The soil physical and hydraulic properties are given in Table 1. In this study, infiltration experiments were carried out by considering three variables, including two soil textures (sandy loam and clay loam), two soil layering (sandy loam in the top layer and clay loam in the bottom and vice versa), and three constant water head sizes (4, 7 and 10 cm). The experiments included 12 treatments and 3 replications, and a randomized complete design was used. Considering 12 treatments and 3 replications, 36 experiments were performed. Analysis of variance of the results was performed using

SPSS software. The characteristics of the treatments are pre- sented in Table 2. For the experiments, four PVC con- tainers with length, width and height of 20 20 70 cm with plexiglass front walls were used.

T A B L E 1 Physical and hydraulic parameters of the studied soils

Soil	Sand (%)	Silt (%)	Clay (%)	Texture	Bulk density (g cm ⁻³)	ρ_s (g cm ⁻³)	K_s (cm min ⁻¹)	θ_i (cm ³ cm ⁻³)	θ_s (cm ³ cm ⁻³)
1	58.1	25.9	16.0	Sandy loam	1.44	2.55	0.09	21.40	40.0
2	20.8	40.2	39.0	Clay loam	1.37	2.65	0.06	20.50	47.2

TABLE 2 Characteristics of the experimental treatments

Row	Treatment	Soil layering	Thickness(cm)	Water head (cm)
1	C4	Clay loam	50	4
2	C7	Clay loam	50	7
3	C10	Clay loam	50	10
4	S4	Sandy loam	50	4
5	S7	Sandy loam	50	7
6	S10	Sandy loam	50	10
7	SC4	Sandy loam (up) and clay loam (down)	25/25	4
8	SC7	Sandy loam (up) and clay loam (down)	25/25	7
9	SC10	Sandy loam (up) and clay loam (down)	25/25	10
10	CS4	Clay loam (up) and sandy loam (down)	25/25	4
11	CS7	Clay loam (up) and sandy loam (down)	25/25	7
12	CS10	Clay loam (up) and sandy loam (down)	25/25	10

To perform each experiment, air-dried soils were sieved through a 2-mm screen. Then, to optimize com- paction and eliminate the effect of initial moisture on the water infiltration rate, the weighted soil moisture reached 15%. For this, the mass of dry soil needed to achieve the specific bulk density and the needed water mass to reach 15% soil moisture were calculated. Then, water was added uniformly to the dry soil.

To achieve a certain bulk density, Proctor's density test apparatus was applied, and the soil was compressed in 5-cm layers with a specified number of strikes (accord- ing to Ma et al., 2010). While filling the soil columns, coarse soil was used 5 cm below each column as a filter to ensure proper drainage. A wire mesh was installed at the end of the column to prevent particles from exiting while water was draining. In the homogeneous treat- ments, the soil columns were filled to a height of 50 cm. Therefore, in two-layered soils, the thickness of each layer was 25 cm. In the upper part of the columns, a space with a height of 15 cm was considered for provid- ing constant water heads by the Mariotte bottle (Figure 1).

After each experiment, the soil was removed from the soil container, and the container was refilled for the next experiment. The types of layering of the soil con- tainers are presented in Figure 2. From right to left, the first container includes sandy loam texture (S treatments), the second includes clay loam texture (C treatments), the third includes two-layer soil, the upper layer is sandy loam and the lower layer is clay loam (SC treatments), and the fourth includes reverse layering (CS treatments).

2.2 | Measurement

Infiltration experiments were carried out in each soil column with water heads of 4, 7 and 10 cm. A Mariotte bottle (with a height and internal diameter of 60 and 16 cm, respectively) was used to provide a constant water head on the soil surface during the infiltration process (Figure 2). First, the Mariotte bottle was filled with water, and the air inside was evacuated using the installed air valve. Then, the inlet valve of the Mariotte bottle to the soil container was opened, and water entered the soil

FIGURE 1 Schematic of the experimental model used for two-layered treatments

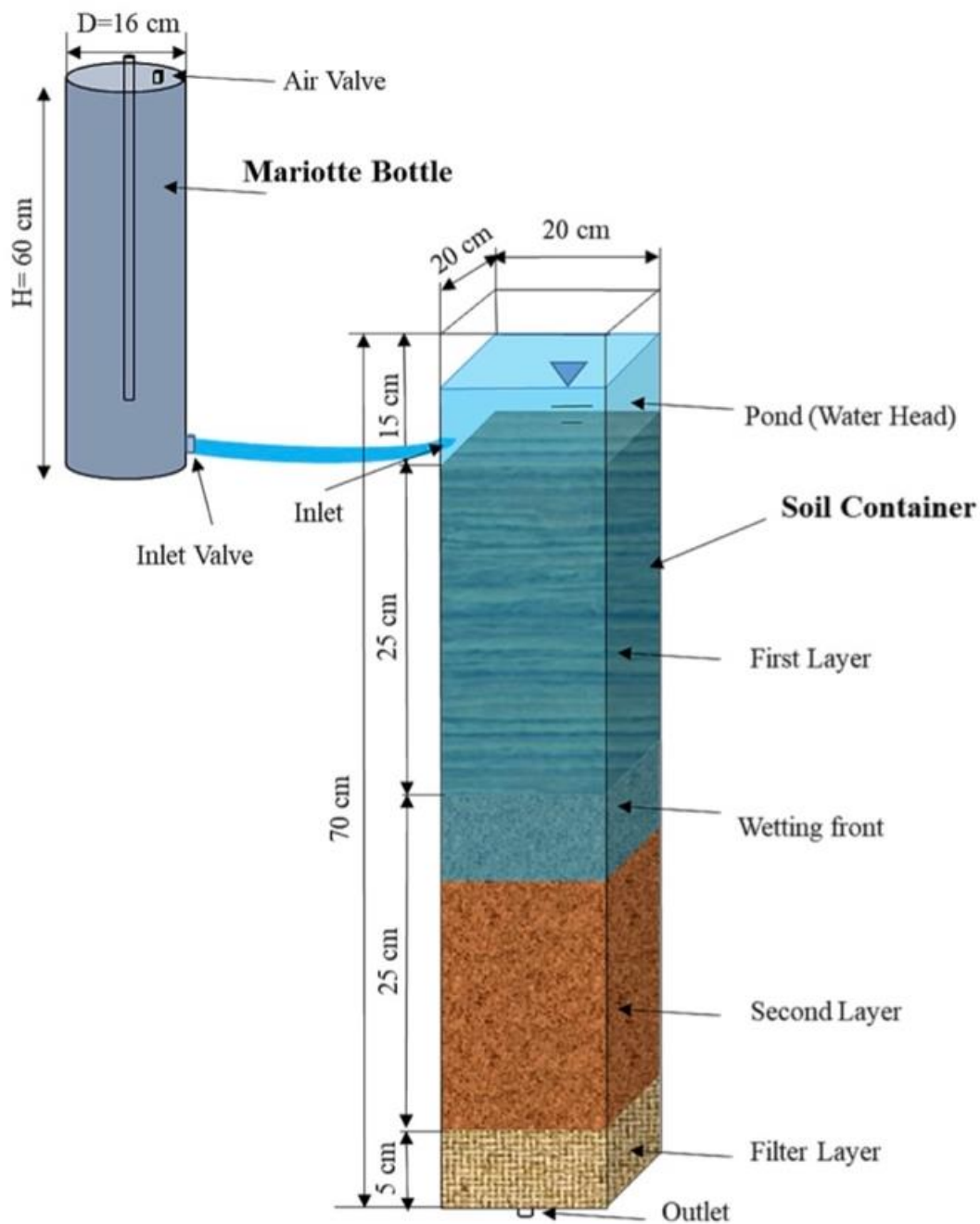


FIGURE 2 The set-up of experiments: (a) the column of sandy loam, (b) the column of clay loam, (c) the column of two-layered soil (sandy loam (up) and clay loam (down)), (d) the column of two-layered soil (clay loam (up) and sandy loam (down)), (e) filter, (f) Mariotte bottle, (g) water head, (h) watermark and (i) wet sensor and (j) soil container



container. Therefore, the water level on the soil increased and reached a constant value. The reading of the water head was continued at different times until a constant water head was created on the soil surface. The ponding formation time varied between 0.5 and 1.8 min in different treatments. In each experiment, to determine the infiltration parameters, the temporal changes in the water level in the Mariotte bottle were read. The experiments were continued until the moisture front reached the end of the soil container.

Since the infiltration velocity is quite large at the early stages of the infiltration process, the water levels in the Mariotte bottle were read over 10, 20, 40 and 60 s and 2,3,5,7,9,11,13,15,18,21,24,27,31 and 35 min, then every 5 min until 60 min, every 8 min until 100 min and every 10 min until 130 min. Of course, in the two-layered soils, the water level was read at the interface of the two layers.

The tensiometers were placed at depths of 5, 15, 25, 35 and 45 cm of the soil in the columns. Therefore, the matric potential at the wetting front, which is one of the parameters of the Green–Ampt model, was read. These tensiometers were installed during soil compaction and filling the columns. Additionally, the initial water contents at different depths (5, 15, 25, 35 and 45 cm) were read using a WET-Sensor (type WET-2, DELTA-T-England). The end time of the experiment varied from 33 to 128 min according to treatments due to differences in soil texture, layering and water head. Because of the

transparency of the soil container glass, the movement of the moisture front was observed. The matric potential was also measured at the interface of the two layers using a watermark (IRROMETER Company, California) of approximately 2 kPa (due to air entry and soil unsaturation).

2.3 | Infiltration models The Kostiakov model (1932):

$$I = at^b \quad (1)$$

where I is the cumulative infiltration [L], t is the time of the test [T] and a [LT^b] and b [] are experimental coefficients that depend on rainfall intensity, initial soil moisture, bulk density, texture and vegetation (Adindu et al., 2014; Parhi, 2014).

The modified Kostiakov model was obtained as (Mezencev, 1948)

$$I = at^b + f_K t \quad (2)$$

where f_K is the final infiltration rate of soil [LT⁻¹], which occurs after a long time and soil saturation.

The Horton model was developed as (Horton, 1940)

$$i = f_c + (f_0 - f_c)e^{-kt} \quad (3)$$

where i is the infiltration rate [LT⁻¹], f_c is the final infiltration rate [LT⁻¹], f_0 represents the initial infiltration rate [LT⁻¹] and k [T⁻¹] is a constant coefficient that relies on the texture and initial moisture of the soil.

The Philip model (1957) was calculated based on the following equation:

$$I = St^{1/2} + At \quad (4)$$

where S is the sorptivity factor [LT^{1/2}], which depends on the initial and final moisture content of the soil, and A is a constant coefficient, which is a function of the initial and final moisture of the soil [LT⁻¹].

The HYDRUS-1D model uses the numerical solution of the one-dimensional Richards equation as follows ((Simunek et al., 2005):

$$\frac{\partial \theta(h,t)}{\partial t} = \frac{\partial}{\partial z} \left[K(h) \left(\frac{\partial h}{\partial z} + 1 \right) \right] \quad (5)$$

where θ is the volumetric moisture content of the soil [L³L⁻³], h is the pressure head [L], Z is the vertical distance from the soil surface [L] and $k(h)$ is the unsaturated hydraulic conductivity [LT⁻¹], which is estimated by van Genuchten et al. (1991):

$$K(h) = \frac{K_s (1 - (\alpha h)^{n-1} [1 + (\alpha h)^n]^{-m})^2}{[1 + (\alpha h)^n]^{ml}} \quad (6)$$

$$m = 1 - \frac{1}{n} \quad (7)$$

where K_s is the soil saturated hydraulic conductivity [LT⁻¹] and n , m , α and l are experimental parameters []. Additionally, to estimate the values of θ_r , the retention curve equation proposed by van Genuchten (1980) was used as

$$\theta = \theta_r + \frac{\theta_s - \theta_r}{(1 + (\alpha h)^n)^m} \quad (8)$$

where θ and θ_r are the soil saturation and residual moisture content, respectively [L³L⁻³]. In this study, empirical soil hydraulic parameters, including n , α and θ_r , were unknown and were obtained with the RETC software (Ma et al., 2010; Schaap et al., 2001). To determine the hydraulic parameters of the model, the obtained values were evaluated, and based on the results, the coefficients were calibrated. The final parameters are presented in Table 3. Additionally, l was considered to be 0.5 (Ma et al., 2010), and two other hydraulic parameters, θ_s and K_s , were measured (Ma et al., 2010). The values of K_s and θ_s are presented in Table 1.

Since the experiments were carried out with a constant head, upper boundary conditions were applied based on the constant pressure head (4, 7 and 10 cm heads) during the test. Additionally, the initial conditions were considered based on constant water content. Down-stream boundary conditions were considered as free drainage. The upstream and downstream boundary conditions in this study were as follows (Ma et al., 2010):

$$h(0,t) = h_0 \quad (9)$$

$$\frac{\partial h}{\partial z} = 0 \quad (10)$$

where h_0 is the constant water potential at the soil surface, and Equation (9) shows that the change in water potential with respect to soil depth is zero (free drainage condition). Additionally, the initial volumetric moisture content of all treatments was approximately 20% (the change in water potential (kPa) and water content (%) during the moving moisture front were approximately (40, 21), (30, 23), (20, 26), (10, 29) and (0, 40)). The Green and Ampt (1911) model considers the flow in the unsaturated zone influenced by soil suction and in the saturated zone influenced by the gravity potential and constant suction head of the moisture front and expresses the infiltration rate in this zone according to Darcy's law as (Green & Ampt, 1911)

$$i = K_s \frac{L_f + S_f + h_0}{L_f} = K_s \left(1 + \frac{S_f + h_0}{L_f} \right) \quad (11)$$

where L_f represents the wetting front thickness [L], S_f is the matric suction of the wetting front [L] that is measured by the watermark and h_0 is the constant head over the soil [L]. The infiltration rate in the soil is obtained from the following equation:

$$i = \bar{K}_s \frac{L_f + S_f + h_0}{L_f} \quad (12)$$

where K_s is the average saturated hydraulic conductivity of the soil, which is described as

$$\bar{K}_s = \frac{\sum_{i=1}^{n+1} D_i}{\sum_{i=1}^{n+1} D_i / K_{s,i}} \quad (13)$$

where $K_{s,i}$ is the saturated hydraulic conductivity in the i th layer [LT⁻¹], D is the thickness of each layer [L] and the subscripts i and n are the soil layer number and the saturation layer number, respectively.

The modified Green–Ampt equation incorporates air entry into the soil column (Ma et al., 2010). To consider the impact of air entrapment, a reduction factor S_a is given:

$$S_a = \frac{S_m}{S_s} = \frac{I + S_i}{S_s} \quad (14)$$

where S_a is the saturation coefficient [], S_m and S_s are the measured moisture content and the total saturated moisture content in the wetted area [L], respectively, S_i is the total initial moisture content [L] and I is the total cumulative infiltration measured [L]. Thus, the actual hydraulic conductivity (k_a) and actual moisture content (θ_a) in the saturation area can be obtained from the following equations:

$$K_a = K_s S_a \quad (15)$$

$$\theta_a = \theta_s S_a \quad (16)$$

The reduction factor S_a and the actual hydraulic conductivity K_a for sandy loam are 0.915 and 0.0823 cm min⁻¹, respectively. Additionally, these parameters for clay loam are 0.843 and 0.0508 cm min⁻¹, respectively.

2.4 | Statistical indicators

Finally, statistical indicators, including the root mean squared error (RMSE), mean absolute error (MAE), per cent bias (PBIAS) and Nash–Sutcliffe coefficient (NS; Nash & Sutcliffe, 1970), were used to compare the accuracy of infiltration models and to choose the best infiltration model according to Equations (17)–(20) (Horn, 1993):

$$\text{RMSE} = \sqrt{\frac{1}{n} \sum_{i=1}^n (S_i - O_i)^2} \quad (17)$$

$$\text{MAE} = \frac{\sum_{i=1}^n (|S_i - O_i|)}{n} \quad (18)$$

$$\text{PBIAS} = \frac{\sum_{i=1}^n (S_i - O_i)}{\sum_{i=1}^n O_i} \quad (19)$$

$$\text{NS} = 1 - \frac{\sum_{i=1}^n (S_i - O_i)^2}{\sum_{i=1}^n (O_i - \bar{O})^2} \quad (20)$$

where S_i , O_i , \bar{O} and n are the simulated data, observed data, average of observed data and total number of observed data, respectively. The RMSE value is always positive, and if it approaches zero, the simulation result will be more accurate. PBIAS represents the percentage difference between simulated and observed data. The positive value of PBIAS represents overestimation, and negative value indicates lower estimation of the model. If the PBIAS value is between 10 and +10%, the simulation result will be highly accurate. The NS shows the accuracy of the data fitness, which is in the range of negative infinity in the worst case up to one in the best simulation state. Finally, the best infiltration model is selected using the ranking method. The ranking method is that each model with the lowest values of RMSE, MAE and PBIAS errors and the highest NS is ranked 1, and the other models are ranked 2 or more. Finally, the total ranking of statistical indicators is calculated for each treatment; then each model with the lowest rank is selected as the best model.

3 | RESULTS AND DISCUSSION 3.1 | The effect of texture and layering

on infiltration rate

In each experiment, the water level of the Marriott bottle was read using a piezometer installed behind it at different times from the beginning of the experiment until the moisture front reached the bottom of the soil container. Then, the water level drop in the Marriott bottle was calculated at different periods. To calculate the volume of water infiltrated into the soil, the water level drop value was multiplied by the cross-sectional area of the Marriott bottle (200.96 cm²), and then the water infiltration depth was calculated by dividing the volume of infiltrated water by the cross-sectional area of the soil container (400 cm²). Finally, the rate of infiltration in each period was calculated by dividing the infiltration depth by the duration of infiltration. According to the

results, at a constant water head, the infiltration rate in both soil textures and both layering arrangements decreased over time (Figure 3). The infiltration rate in sandy loam was higher than that

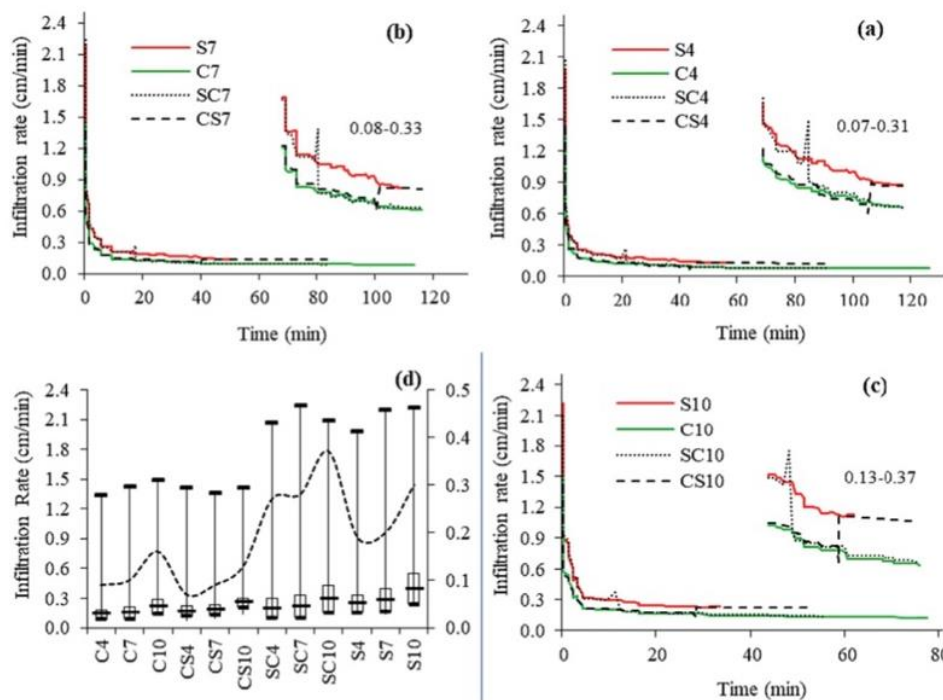


FIGURE 3 (a)–(c) The effect of soil texture and layering on the variations in the measured infiltration rate at three heads of 4, 7 and 10 cm: to better show the difference in infiltration rate in homogeneous treatments and its changes at the two-layer interface in layered soils, the infiltration rate was plotted in small blocks (near a depth of 25 cm). Additionally, (d) box plot of the infiltration rate shows more clearly the trend of infiltration changes with different treatments (the dashed line shows the infiltration rate at a 25 cm depth)

in clay loam soil, and the variations in infiltration rate in both heavier and lighter soils were similar. However, in the SC treatments, the infiltration rate at the two-layer interface was significantly higher than that at the low-permeability bottom layer. So, a jump was observed at the two-layer interface in their infiltration curves. This increase is due to the high matric potential of the lower layer, which consequently increased the hydraulic gradient and infiltration rate according to Darcy's law. Additionally, Mohammadzadeh-Habili and Heidarpour (2015) pointed to a vertical increase in infiltration rate through the passage of the light-to-heavy layer and the reduction of the infiltration rate on the heavy layer. In these treatments (SC), the infiltration rate of the second layer decreases due to the low hydraulic conductivity. However, the infiltration rate in the CS treatments at the two-layer interface was lower than the final infiltration rate in the second layer. This decrease is also due to the low matric potential of the second layer, and finally, according to Darcy's law, reducing the hydraulic gradient decreases the infiltration rate (Mohammadzadeh-Habili & Heidarpour, 2015). In these treatments, because of the higher hydraulic conductivity of the second layer, the flow resistance is low, and the infiltrated water will easily move in the second layer. On the other hand, since the infiltration rate in the second layer is greater than that in the first, after the reduction at the two-layer interface, the infiltration rate clearly increased and approached the final infiltration rate of the light soil. Then, the infiltration

rate decreases again over time. Mohammadzadeh-Habili and Heidarpour (2015) also pointed to the decrease in infiltration rate at the two-layer interface, with the placement of the heavy layer above the light one. The change in infiltration rate at the interface of the two layers can be due to differences in the physical properties of soil, such as texture and structure (Ma et al., 2010). Furthermore, with all water heads, soil texture had a significant influence on the end time of the experiment, while soil layering had little effect on this factor. The end times of the experiments in the SC and CS treatments are similar at a constant head.

According to Figure 3, the sections with clear variations in infiltration are presented accurately in the small blocks. Based on this analysis, it was found that these changes occurred more at the two-layer interface in heterogeneous treatments. Additionally, to compare and accurately show the infiltration rate in homogeneous treatments, changes in the infiltration rate were shown in the middle of the layer (soil depth of 25 cm) in these small blocks. As shown in Figure 3(a), the infiltration rate values at the soil depth of 25 cm in the S4 and C4 treatments and at the two-layer interface (soil depth of 25 cm) in the SC4 and CS4 treatments were 0.19, 0.09, 0.27 and 0.07 cm min^{-1} , respectively, which indicates a 52% increase in infiltration rate in the S4 treatment compared to the C4 treatment (texture effect on infiltration rate) and a 74% increase at the two-layer interface in the SC4 treatment compared to the CS4 treatment (effect of layering on infiltration rate). On the other hand, in the SC4 treatment, by moving the wetting front of the upper layer (high-permeable layer) into the lower layer (lower-permeable layer) due to the high matric suction of the second layer, the infiltration rate at the two-layer interface increased by 42.1%. This jump appears in Figure 3(a). In the case of the CS4 treatment, the infiltration rate at the two-layer interface decreases by 22.2% due to the lower matric suction of the highly permeable second layer. Then, the infiltration rate increases again to reach the final infiltration capacity of the second layer, and these changes are shown in Figure 3(a). The variations in the infiltration rate in Figures 3(b) and (c) are also similar, and only the percentage change in infiltration rate is less than that in Figure 3(a). According to Figure 3(b), the infiltration rate values at the soil depth of 25 cm in the S7 and C7 treatments and at the two-layer interface (soil depth of 25 cm) in the SC7 and CS7 treatments were 0.2, 0.1, 0.28 and 0.09 cm min^{-1} , respectively, which indicates a 50% increase in the S7 treatment compared to the C7 treatment and a 66.7% increase at the two-layer interface in the SC7 treatment compared to the CS7 treatment. In the SC7 treatment, the infiltration rate at the interface of the two layers increased by 35%, and in the CS7 treatment it decreased by 10%. Additionally, according to Figure 3(c), the infiltration rate values at the soil depth of 25 cm in the S10 and C10 treatments and at the two-layer interface in the SC10 and CS10 treatments were 0.3, 0.16, 0.37 and 0.13 cm min^{-1} , respectively, which indicates a 46.7% increase in infiltration rate in the S4 treatment compared to the C4 treatment and a 64.9% increase at the two-layer interface in the SC10 treatment compared to the CS10 treatment. In the SC10 treatment, the infiltration rate at the two-layer interface increased by 23.3%, and in the CS10 treatment, it decreased by 18.8%. Additionally, to accurately show the variations in infiltration rate, a box plot was plotted, as shown in Figure 3(d). Changes in infiltration rate at different heads appear in this figure. Additionally, the dotted diagram of Figure 3(d) shows the infiltration rate at 25 cm

depth and the two-layer interface for homogeneous and heterogeneous treatments, respectively.

3.2 | The effect of water head on infiltration rate

Changes in infiltration rate due to changes in water head over the soil for homogeneous and heterogeneous soils are presented in Figure 4. According to Figure 4, in both the single- and two-layered soil treatments, the infiltration rate increases with increasing water head, which is similar to the results of Al-Ghazal (2002), Al Shakerchy (2009) and Hsu et al. (2017). The infiltration rates of the S4, S7 and S10 treatments were in the intervals of (0.13– 1.98), (0.14–2.2) and (0.23–2.2) cm min^{-1} , respectively; for the C4, C7 and C10 treatments they were in the intervals of (0.075– 1.34), (0.09–1.43) and (0.13–1.49) cm min^{-1} , respectively; for the SC4, SC7 and SC10 treatments they were in the intervals of (0.08–2.07), (0.09–2.24) and (0.14–2.09) cm min^{-1} , respectively; and for the CS4, CS7 and CS10 treatments they were in the intervals of (0.12–1.42), (0.13– 1.36) and (0.22–1.42) cm min^{-1} , respectively. Over time, the infiltration rate decreased. The results showed that the intensity of the decreasing infiltration rate decreased with increasing water head. To better show changes in the infiltration rate in homogeneous treatments, the infiltration rate was plotted in small intervals in small blocks. Additionally, in heterogeneous treatments, due to the clear variation in the infiltration rate at the two-layer interface, infiltration rates were plotted near the interface of the two layers. According to Figure 4, there is little difference between the infiltration rates at the heads of 4 and 7 cm in all treatments. However, there is a clear difference between the infiltration rates at the 7- and 10-cm heads. At different water heads, the process of changes in the infiltration rate at the interface of the two layers was similar, so that in the SC treatments, a jump and then a decrease in the infiltration rate were observed. In the CS treatments, the infiltration rate first decreased and then increased. According to Figure 4(c), the infiltration rates at the two-layer interface in the SC4, SC7 and SC10 treatments were 0.27, 0.28 and 0.37 cm min^{-1} , respectively. In other words, the increase in infiltration rate in the SC7 treatment was 3.7% relative to SC4 and 32.1% in SC10 compared to SC7. Additionally, according to Figure 4(d), the infiltration rate values at the two-layer interface in the CS4, CS7 and CS10 treatments were 0.07, 0.092 and 0.13 cm min^{-1} , respectively. In other words, the infiltration rate was 2.86% higher in the CS7 treatment than in the CS4 treatment and 44.4% higher in the CS10 treatment than in the CS7 treatment. The time of arrival of the wetting front at the interface of the two

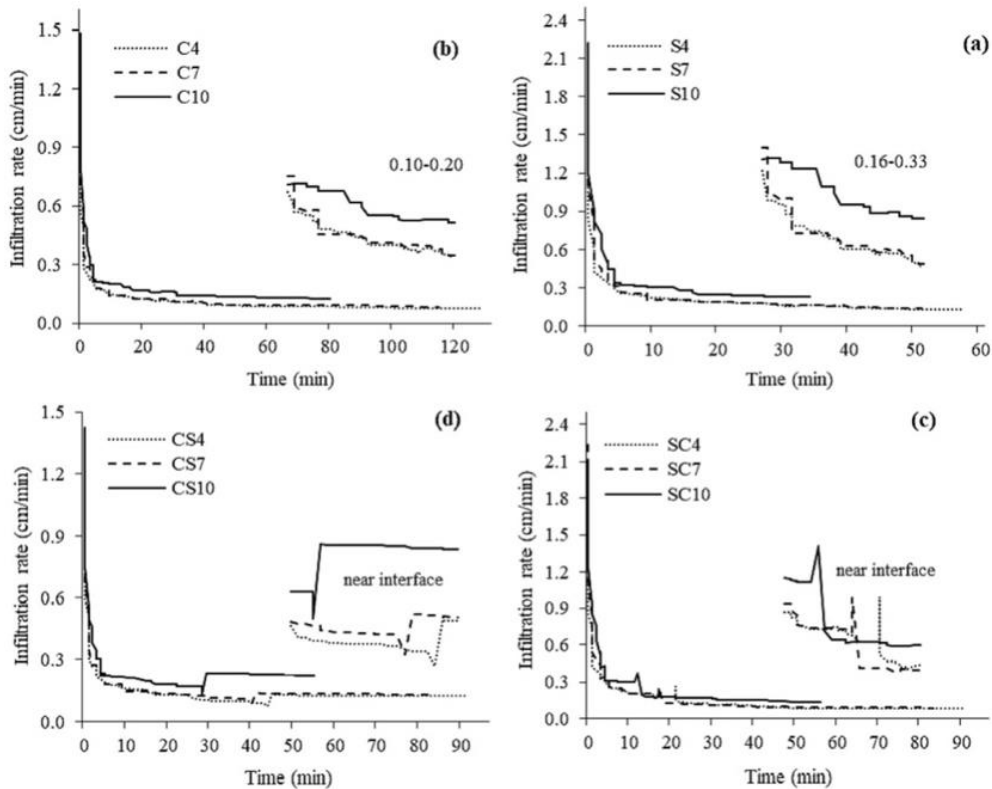


FIGURE 4 The effect of water head on the variations of measured infiltration rate in different textures and layering: to better show the difference of infiltration rate in homogeneous treatments and its changes at the two-layer interface in layered soils, the infiltration rate has been plotted in small blocks (near the depth of 25 cm)

layers had the same procedure, so in the SC4, SC7 and SC10 treatments it was 21, 17 and 11.5 min, respectively, and in the CS4, CS7 and CS10 treatments it was 43, 40 and 28.5 min, respectively. Aronovici (1955) showed that the infiltration rate increases directly with increasing water head. Al Shakerchy (2009) reported a great efficacy of water head on infiltration rate. Additionally, Hsu et al. (2017) showed that cumulative infiltration increases uniformly as head increases.

3.3 | The effect of water head on infiltration models in homogeneous soils

The simulated infiltration rates using empirical and semi-empirical models, including Kostiakov, modified Kostiakov and Horton, and physical models, including Philip, traditional and modified Green–Ampt models and HYDRUS-1D, are presented in Figure 5 for the six homogeneous soil treatments. According to Figure 5, the simulation results of all infiltration models, especially the modified Green–Ampt and modified Kostiakov models, converged with simulated data. To better illustrate the results, the variations were plotted in smaller intervals of infiltration. The percentage of variations in the simulated infiltration rates relative to the measured values (PBIAS) was obtained for homogeneous soils (S and C treatments); then, the average PBIAS value was calculated for each infiltration model and HYDRUS-1D. According to the results, the mean values of PBIAS in the Horton, HYDRUS-1D, Kostiakov, Philip, modified Green–Ampt, modified Kostiakov and traditional Green–Ampt models were equal to 9.67, 7, 3.19, 2.88, 1.36, 0.81 and 7.22%, respectively. The negative and positive values represent lower estimation and overestimation,

respectively. Additionally, the simulation results of the infiltration rate in homogeneous soil treatments often showed that all the equations and the HYDRUS-1D model at the end times and the Kostiakov equation at the mid-infiltration times of the experiments accurately simulate the infiltration rate. Additionally, the standard deviation values of the measured and simulated infiltration rates were

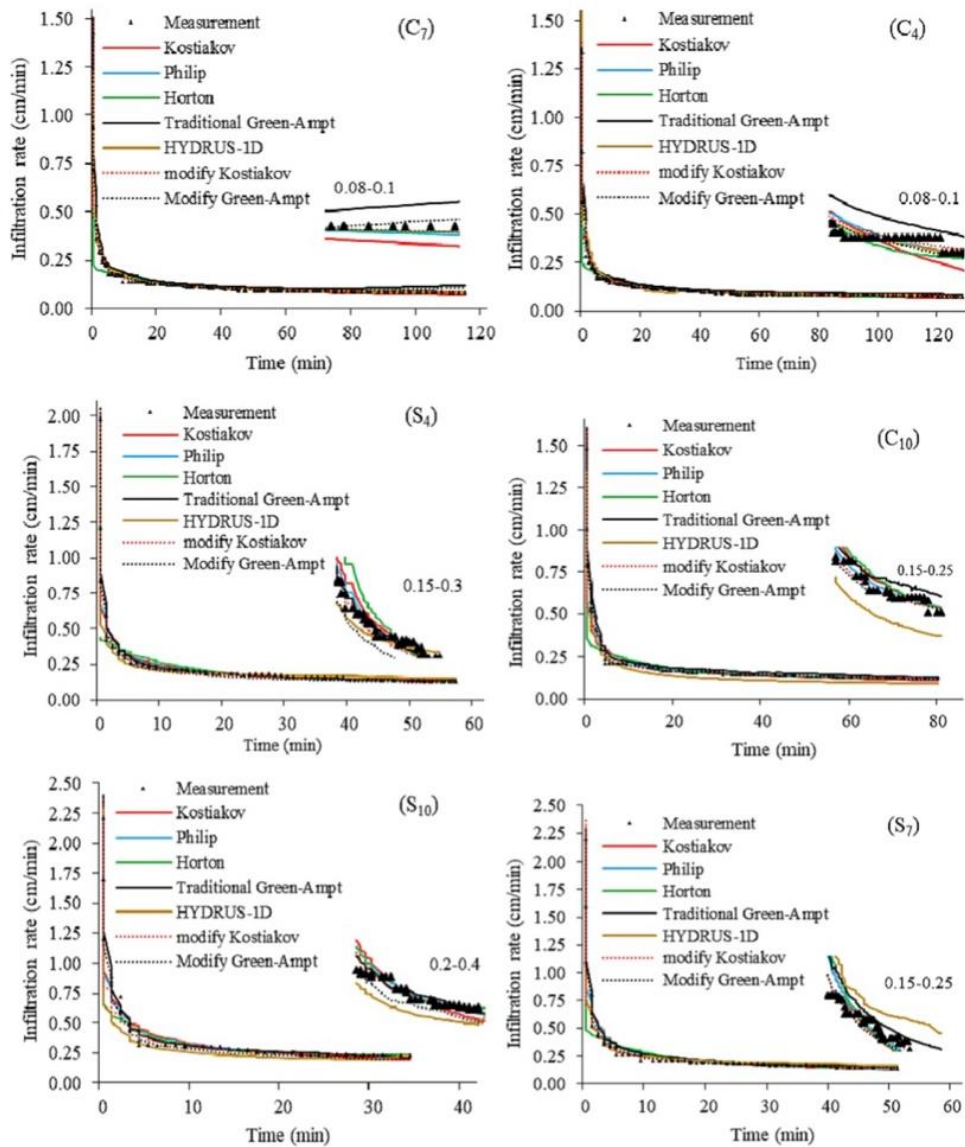


FIGURE 5 Simulation of infiltration rate in homogeneous soil treatments using empirical, semi-empirical and physical equations and the HYDRUS-1D model: to better show the difference in infiltration rate in different models, the infiltration rate has been plotted in small blocks at smaller ranges of infiltration rate (near the depth of 25 cm)

calculated. The values of the standard deviation of the measured data were 0.226 cm min⁻¹. The values of the standard deviation of the simulated data by the Horton, Kostiakov, Philip, HYDRUS-1D, modified Kostiakov and modified and traditional Green-Ampt models were 0.107, 0.164, 0.174, 0.206, 0.219, 0.232 and 0.249 cm min⁻¹, respectively.

The coefficients of the equations were derived based on the measured data and best-fit regression line or curve

(Abdulkadir et al., 2011; Furman et al., 2006; Harisuseno & Cahya, 2020). To estimate the coefficients of the Kostiakov, modified Kostiakov, Horton and Philip models, regression analysis was used so that the fitted equations had the highest coefficient of determination (R^2) and the lowest RMSE. Therefore, the a and b coefficients in the Kostiakov and modified Kostiakov models, the k and f_0 coefficients in the Horton model and the S and A coefficients in the Philip model were derived

15310361, 2024, 3, Downloaded from
<https://onlinelibrary.wiley.com/doi/10.1002/ird.2918> by Faculdade Medicina De Lisboa, Wiley Online Library on [22/01/2025]. See the Terms and Conditions (<https://onlinelibrary.wiley.com/terms-and-conditions>) on Wiley Online Library for rules of use; OA articles are governed by the applicable Creative Commons License

from the slope and intercept of the fitted lines. However, considering that the modified Kostiakov and Horton models had three unknown coefficients, the f_k and f_c coefficients (respectively, in these models) were estimated by trial and error (considering the best-fit regression). Additionally, all the parameters of the traditional and modified Green–Ampt models, including the wetting front thickness (L_f), the saturated hydraulic conductivity of the soil layers (K_s) and the matric suction of the wetting front (S_f), were measured. To increase the accuracy of the results, instead of using the Brooks and Corey (1964) retention curve to estimate the bubbling pressure (h_b), which is one of the main parameters of the S_f equation, the value of S_f was measured using a watermark. Additionally, as mentioned in Section 2.3, in the modified Green–Ampt model, the coefficient K_a is used instead of K_s (Equation (15)), which is estimated using K_s and S_a , and the value of S_a was also estimated by the measured moisture content and the total saturated moisture content in the wetted area (Equation (14)). The calculated parameters of the Kostiakov, modified Kostiakov, Philip and Horton models in homogeneous soil treatments are presented in Table 4. According to Table 4, the values of infiltration coefficients in the S treatment are often higher than those in the C treatment.

The statistical indicators were calculated to estimate the most accurate infiltration model in homogeneous soil treatments. The values of statistical indicators (MAE, NS, PBIAS and RMSE) and rankings of infiltration models for homogeneous soil treatments are given in Table 5. According to the total ranking, the modified Green–Ampt infiltration model was selected as the best infiltration model in all homogeneous soil treatments (Table 5). Additionally, the modified Kostiakov model ranked second in all treatments except S_7 . On average, the traditional Green–Ampt model and HYDRUS-1D had better results. The Philip and Kostiakov models had weaker results, and the Horton model had the lowest rank. Ma et al. (2016) also showed that the Green–Ampt equation can simulate infiltration parameters. Additionally, Mao et al. (2016) confirmed the high accuracy of the modified Green–Ampt model in a horizontal soil column. Researchers such as Gifford (1976), Hajabbasi (2006) and Haghghi et al. (2010) found that the Horton equation has better fitness with observed data. Researchers such as Navar and Synnott (2000) found a high accuracy of the modified Kostiakov model in the simulation of infiltration rate, and Machiwal et al. (2006) and Oku and Aiye-lari (2011) reported a high accuracy of the Philip model. Chari et al. (2020) and Jha et al. (2019) noted that the precision of the modified Kostiakov model is greater than that of the Philip model in

estimating infiltration based on double rings. In other words, a comparison of this study's results with previous studies suggests that each infiltration model, under certain conditions, simulates the infiltration process better than others (Sihag et al., 2017; Turner, 2006), which is due to the nature of the variability of soil hydraulic characteristics, especially hydraulic conductivity, even in similar soil units (Comegna & Vitale, 1993; Nielsen et al., 1973). In addition, according to Table 5, the accuracy of infiltration models in the clay loam texture has been higher than that of sandy loam. In most of the treatments, the accuracy of infiltration models decreased with increasing water head. The greatest effect of the water head was observed on the results of the HYDRUS-1D, modified Kostiakov and modified Green–Ampt models. The least effect of the water head was related to the Kostiakov and Philip models. Additionally, Philip and Horton's models have similar accuracy in estimating the infiltration rate at water heads of 7 and 10 cm, but the accuracy of these models' estimation results at a water head of 7 cm is lower than that at a water head of 4 cm. In the modified Green–Ampt, the difference in the accuracy of the model estimation for water heads of 7 and 10 cm was considerable.

TABLE 4 Calculated parameters of the Kostiakov, modified Kostiakov, Philip and Horton models in homogeneous soil treatments of C and S

Treatment	Kostiakov		Modified Kostiakov			Horton			Philip	
	<i>a</i>	<i>b</i>	<i>a</i>	<i>b</i>	<i>f_k</i>	<i>f₀</i>	<i>f_c</i>	<i>k</i>	<i>A</i>	<i>S</i>
C4	0.3816	-0.3556	0.4134	-0.6502	0.0600	0.2300	0.0750	-0.0451	0.0423	0.7348
C7	0.4288	-0.3777	0.4429	-0.6577	0.0640	0.2061	0.0825	-0.0382	0.0436	0.7867
C10	0.5215	-0.3581	0.4795	-0.6301	0.0950	1.0614	0.1250	-1.5638	0.0702	0.9161
S4	0.5998	-0.3863	0.5753	-0.6781	0.1030	0.4416	0.1300	-0.0807	0.0608	1.1124
S7	0.7248	-0.4385	-0.6660	0.6882	0.0940	0.4810	0.1340	-0.0832	0.0269	1.5217
S10	0.8628	-0.4159	-0.6186	0.7344	0.1360	0.6515	0.2280	-0.1539	0.0851	1.5079

TABLE 5 The values of statistical indicators and ranking of Kostiakov, modified Kostiakov, Philip, Horton, traditional and modified Green-Ampt models and HYDRUS-1D in homogeneous soil treatments of C and S

Model	Treatment	MAE (cm min ⁻¹)	NS (-)	PBIAS (%)	RMSE (cm min ⁻¹)	Sum rank	Total rank
Kostiakov	C4	0.0170	0.7861	-3	0.0648	24	6
	C7	0.0210	0.8148	-4	0.0695	23	6
	C10	0.0270	0.8567	-3	0.0694	21	5
	S4	0.0299	0.8237	-3	0.0995	21	6
	S7	0.0370	0.9225	0	0.1052	21	6
	S10	0.0509	0.9130	-3	0.1031	18	5
Modified Kostiakov	C4	0.0085	0.9845	0	0.0174	9	2
	C7	0.0091	0.9766	-1	0.0247	8	2
	C10	0.0130	0.9720	-1	0.0306	8	2
	S4	0.0162	0.9860	0	0.0323	9	2
	S7	0.0213	0.9616	-1	0.0583	16	4
	S10	0.0343	0.9513	-2	0.0749	11	3
Horton	C4	0.0200	0.7423	-7	0.0711	28	7
	C7	0.0310	0.6237	-13	0.0991	27	7
	C10	0.0360	0.6751	-8	0.0996	25	7
	S4	0.0399	0.6896	-6	0.1320	27	7
	S7	0.0565	0.6210	-10	0.1831	28	7
	S10	0.0457	0.6716	-11	0.1944	25	7
Philip	C4	0.0100	0.8968	-3	0.0450	19	5
	C7	0.1500	0.8824	-4	0.0550	19	5
	C10	0.0190	0.9208	-3	0.0520	15	4
	S4	0.0232	0.8985	-2	0.0760	16	4
	S7	0.0325	0.9337	0	0.0960	17	5
	S10	0.0432	0.9206	-3	0.0960	17	4
Traditional Green-Ampt	C4	0.0017	0.9400	1	0.0343	12	3
	C7	0.0021	0.9640	13	0.0306	16	4
	C10	0.0023	0.9480	10	0.0418	15	3
	S4	0.0015	0.9840	3	0.0301	11	3
	S7	0.0027	0.9840	9	0.0369	12	2
	S10	0.0027	0.9790	4	0.0494	9	2
Modified Green-Ampt	C4	0.0006	0.9850	1	0.0169	6	1
	C7	0.0008	0.9940	2	0.0126	5	1
	C10	0.0009	0.9930	-0	0.0155	4	1
	S4	0.0019	0.9900	-5	0.0230	9	1
	S7	0.0012	0.9960	-0	0.0180	4	1
	S10	0.0029	0.9880	-6	0.0364	9	1
Hydrus-1D	C4	0.0147	0.9400	3	0.0143	14	4
	C7	0.0116	0.9460	-3	0.0380	14	3
	C10	0.0412	0.9070	-18	0.0561	24	6
	S4	0.0286	0.9280	-6	0.0644	20	5
	S7	0.0265	0.9640	-1	0.0565	14	3
	S10	0.0742	0.7800	-15	0.1406	25	6

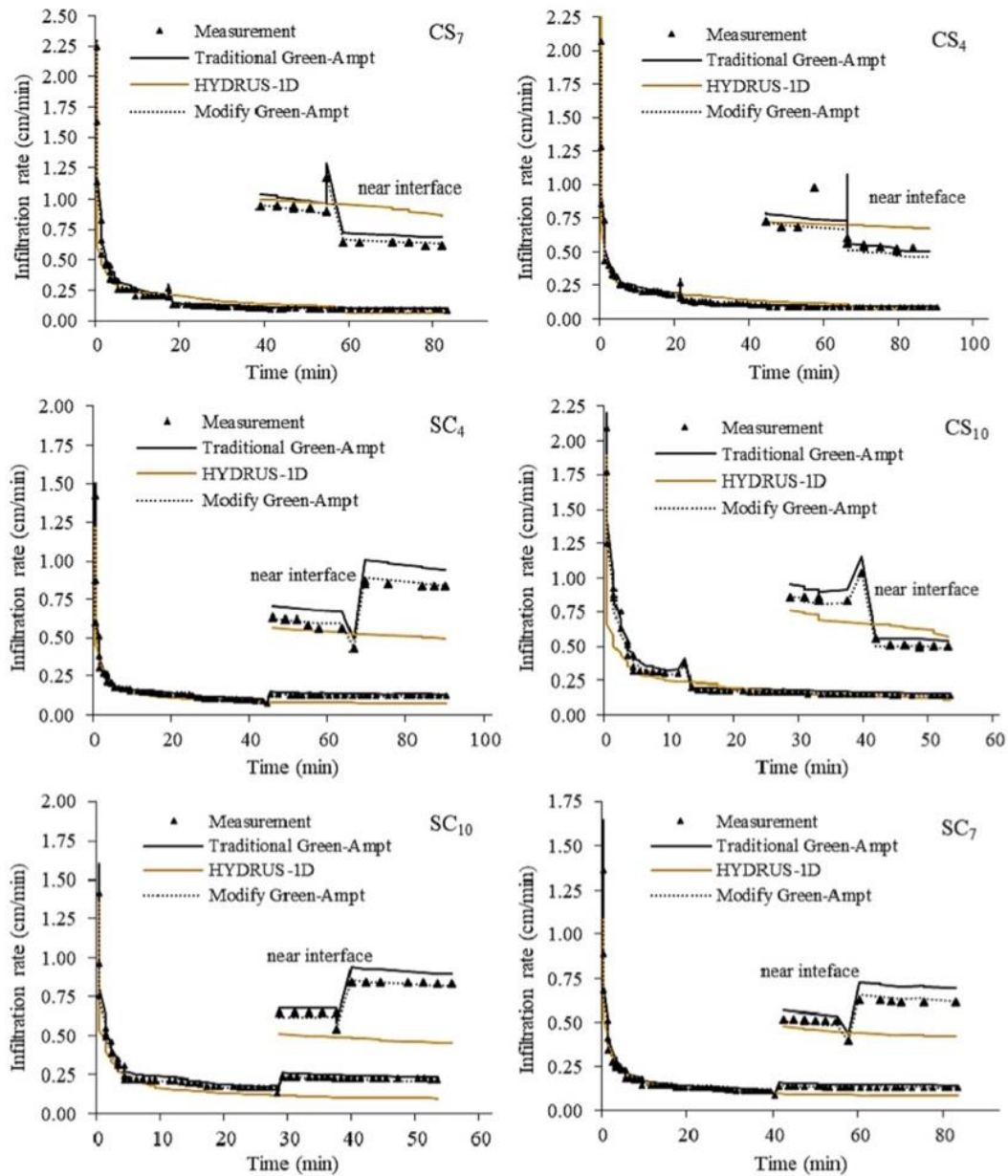


FIGURE 6 Simulation of infiltration rate in heterogeneous soil treatments using traditional and modified Green–Ampt models and HYDRUS-1D: to better show the difference in infiltration rate at the interface of the two layers in different models, the infiltration rate has been plotted in small blocks at smaller ranges of infiltration rate (near the interface of two layers)

3.4 | The effect of water head on the infiltration models in the layered soils

The simulated infiltration rates in heterogeneous soils (SC and CS treatments) using HYDRUS-1D and traditional and modified Green–Ampt models are presented in Figure 6. According to Figure 6, the traditional and modified Green–Ampt equations can predict the infiltration rate increase at the two-layer interface in SC treatments and can also reduce the infiltration rate in CS treatments. This result is completely consistent with the results of Mohammadzadeh-Habili and Heidarpour (2015). On the other hand, the modified Green–Ampt has more convergence with observed data due to the consideration of air entry values. However, the HYDRUS-1D model could not predict the variation in infiltration rate at the two-layer interface. The results of this section are in

agreement with those of researchers such as Moore and Eigel (1981), Wang et al. (1999), Liu et al. (2008), Ma et al. (2010) and Mohammadzadeh-Habili and Heidar-pour (2015), who showed that the modified Green–Ampt equation properly predicts the infiltration process in layered soils. In Figure 6, to better show the results, the infiltration rates near the interface of two layers were plotted in small blocks. The average PBIAS of the heterogeneous soils (SC and CS treatments) for the modified and traditional Green–Ampt models and HYDRUS-1D were 0.94, 9.39 and 10.59%, respectively. The values indicate the ignored lower estimation of the modified Green–Ampt equation, the overestimation of the traditional Green–Ampt equation and the lower estimation of the HYDRUS-1D model in this study. To determine the most accurate infiltration model in heterogeneous soils, the values of statistical indicators (MAE, NS, PBIAS and RMSE) of the traditional and modified Green–Ampt models and HYDRUS-1D were calculated and are

TABLE 6 Values of statistical indicators of traditional and modified Green–Ampt models and HYDRUS-1D in heterogeneous treatments

Model	Treatment	MAE (cm min ⁻¹)	NS (-)	PBIAS (%)	RMSE (cm min ⁻¹)	Sum rank	Total rank
Traditional Green–Ampt	SC4	0.0016	0.9871	6	0.0277	9	2
	SC7	0.0025	0.9870	11	0.0327	9	2
	SC10	0.0030	0.9840	9	0.0409	9	2
	CS4	0.0016	0.9791	8	0.0229	7	2
	CS7	0.0021	0.9302	11	0.042	9	2
	CS10	0.0024	0.9541	9	0.0373	8	2
Modified Green–Ampt	SC4	0.0013	0.9901	-3	0.0236	4	1
	SC7	0.0086	0.9970	1	0.0155	5	1
	SC10	0.0011	0.9951	-0	0.0232	4	1
	CS4	0.0007	0.9910	-2	0.0149	4	1
	CS7	0.0009	0.9830	0	0.0206	4	1
	CS10	0.0010	0.9910	-1	0.0162	4	1
Hydrus-1D	SC4	0.0329	0.9230	3	0.0519	11	3
	SC7	0.0511	0.8511	0	0.0968	10	3
	SC10	0.0448	0.8490	-9	0.0866	11	3
	CS4	0.0300	0.9072	-16	0.0485	12	3
	CS7	0.0278	0.9070	-12	0.0486	11	3
	CS10	0.0729	0.6350	-29	0.0878	12	3

TABLE 7 The results of variance analysis of texture, layering and water head at 0, 10, 20 and 30 min at the 5% probability level

Source of variation	df	T = 0 min		T = 10 min		T = 20 min		T = 30 min	
		MS × (10 ⁻⁴)	Sig.	MS × (10 ⁻⁴)	Sig.	MS × (10 ⁻⁴)	Sig.	MS × (10 ⁻⁴)	Sig.
Texture	1	15696.3	0.003*	14700.0	0.002*	5633.3	0.058 ^{ns}	1408.3	0.213 ^{ns}
Layering	1	3.0	0.826 ^{ns}	0.1	1.000 ^{ns}	1200.0	0.209 ^{ns}	1008.3	0.267 ^{ns}
Ponding depth	2	37.3	0.563 ^{ns}	7308.3	0.003*	2925.0	0.109 ^{ns}	7033.3	0.058 ^{ns}
Texture*Layering	1	3.0	0.826 ^{ns}	300.0	0.074 ^{ns}	2133.3	0.135 ^{ns}	5208.3	0.074 ^{ns}
Texture*Ponding Depth	2	4.3	0.917 ^{ns}	475.0	0.051 ^{ns}	108.3	0.768 ^{ns}	233.3	0.650 ^{ns}
Layering*Ponding Depth	2	243.0	0.165 ^{ns}	25.0	0.500 ^{ns}	175.0	0.672 ^{ns}	433.3	0.500 ^{ns}
Error	2	48.0		25.0		358.3		433.3	
Corrected total	11								

Note: * and ns show the significant and insignificant effect of factors.

TABLE 8 The results of variance analysis of texture, layering and water head at 50, 70 and 90 min at the 5% probability level

Source of variation	df	T = 50 min		T = 70 min		T = 90 min	
		MS × (10 ⁻⁴)	Sig.	MS × (10 ⁻⁴)	Sig.	MS × (10 ⁻⁴)	Sig.
Texture	1	75.0	0.789 ^{ns}	75.0	0.759 ^{ns}	133.3	0.705 ^{ns}
Layering	1	8.3	0.928 ^{ns}	8.3	0.918 ^{ns}	33.3	0.848 ^{ns}
Ponding depth	2	5 858.3	0.121 ^{ns}	6 775.0	0.082 ^{ns}	7 033.3	0.091 ^{ns}
Texture*Layering	1	10 208.3	0.071 ^{ns}	11 408.3	0.049*	10 800.0	0.059 ^{ns}
Texture*Ponding Depth	2	25.0	0.970 ^{ns}	25.0	0.961 ^{ns}	33.3	0.955 ^{ns}
Layering*Ponding Depth	2	8.3	0.990 ^{ns}	58.3	0.913 ^{ns}	33.3	0.955 ^{ns}
Error	2	808.3		608.3		700.0	
Corrected total	11						

Note: * and ns show the significant and insignificant effects of factors.

presented in Table 6. According to Table 6, the modified Green–Ampt equation with the lowest rank in all SC and CS treatments is seen as the best infiltration model. Next, the traditional Green–Ampt model and HYDRUS-1D were ranked 2 and 3, respectively. In layered soil, the accuracy of the HYDRUS-1D and Green–Ampt models was higher than in homogeneous soil. Additionally, the accuracy of the mentioned models usually decreases with increasing water head. The effect of the water head on the simulation accuracy of the HYDRUS-1D model was greater than that of the Green–Ampt model.

3.5 | The combined effect of texture, layering and water head on infiltration rate

The P-value and MS (“Mean Square” in the SPSS software) of the measured data were determined using SPSS software, and the results are presented in Tables 7 and 8. Analysis of variance was performed using a three-factor test. F was related to the main effects, and the dual interactions were obtained using triple interactions (according to the research of Pirzad et al., 2011). Analysis of variance was performed at 0, 10, 20, 30, 50, 70 and 90 min due to the end time of tests in different treatments. The results of variance analysis at the start time showed a significant difference between the two levels of soil texture. Other factors of layering, water head and the interaction between them, and the interaction between them and soil texture, were not significant. Additionally, the analysis result at 10 min showed that the effect of the two factors of texture and water head was significant. However, the interaction effect between these two factors, the layering effect and the interaction effect between layering and the other two factors were not. The interaction effect between soil texture and soil layering was significant at 70 min. However, the effect of the main parameters and the interaction effect between the water head and two other factors were not. For other times of 20, 30, 50 and 90 min, the effect of the main factors and the interaction between them was insignificant.

4 | CONCLUSION

Irrigation is often performed without specific knowledge of soil water infiltration, water head and deep percolation losses. But these parameters are essential in the irrigation efficiency of traditional irrigation methods (especially in arid and semi-arid regions). Therefore, we studied the impact of soil texture, layering and three water heads (4, 7 and 10 cm) on the water infiltration rate. As expected, both sandy loam and clay loam textures had similar infiltration rate variations over time. In the SC treatments, the infiltration rate at the two-layer interface increased due to increased suction from the

lower layer. Then, it decreased when the wetting front entered the second layer. In the CS treatments, the infiltration rate at the two-layer interface decreased due to the lower suction of the second layer, but it increased again to approximately the final infiltration capacity of the second layer. In both the homogeneous and heterogeneous soil treatments, the infiltration rate increased with increasing water head. Additionally, there was a slight difference between the infiltration rates at water heads of 4 and 7 cm in all treatments, while there was a clear difference between the 7- and 10-cm heads. The analysis of variance showed that only the effect of soil texture at the start of the experiment and at 10 min and the effect of water head at 10 min were significant. The effect of layering at any time was not significant. Regarding the combined effect, only the interaction effect between soil texture and soil layering was significant at 70 min. The modified Green–Ampt was shown to be the most accurate infiltration model for both homogeneous and heterogeneous soils. Therefore, we recommend its use at the catchment area level. The accuracy of infiltration models in the heavier texture was greater than that in the lighter, and it decreased with increasing water head in most treatments. In the homogeneous soils, the maximum effect of the water head was observed in the results of the HYDRUS-1D, modified Kostikov and modified Green–Ampt models. The least effect was related to the Kostikov and Philip models. Additionally, in heterogeneous soils, the accuracy of the infiltration models in the CS treatments was higher, and it usually decreased with increasing water head. In addition, the effect of water head on the results of the HYDRUS-1D model was greater than that of the Green–Ampt model.

ACKNOWLEDGEMENTS

This research was supported by funds from the Urmia University.

DATA AVAILABILITY STATEMENT

Data available on request from the authors

REFERENCES

- Abdulkadir, A., Wuddivira, M.N., Abdu, N. & Mudiare, O.J. (2011) Use of Horton infiltration model in estimating infiltration characteristics of an alfisol in the northern Guinea savanna of Nigeria. *Agricultural Science and Technology*, 1, 925–931.
- Adindu, R.U., Akoma, C.S. & Igbokwe, K.K. (2014) Estimation of Kostikov's infiltration model parameters of some sandy loam soils of Ikwuano – Umuahia, Nigeria. *Open Transactions on Geosciences*, 1(1), 34–38.
- Adindu, R.U., Igbokwe Kelechi, K. & Dike, I.I. (2015) Philip model capability to estimate infiltration for Solis of ab, Abia state. *Earth Sciences and Geotechnical Engineering*, 5(2), 63–68.
- Al Shakerchy, M.S.M. (2009) Effect of water head on the infiltration characteristics by using the laboratory tests. *Al-Qadisiyah Journal for Engineering Sciences*, 2(4), 705–721.
- Al-Ghazal, A.A. (2002) Effect of ripping and water head on infiltration rate of soils in Saudi Arabia. *Pakistan Journal of Biological Sciences*, 5(3), 263–265. Available from: <https://doi.org/10.3923/pjbs.2002.263.265>

- Ali, S., Islam, A., Mishra, P.K. & Sikka, A.K. (2016) Green-Ampt approximations: a comprehensive analysis. *Journal of Hydrology*, 535, 340–355. Available from: <https://doi.org/10.1016/j.jhydrol.2016.01.065>
- Aronovici, V.S. (1955) Model study of ring infiltrometer performance under low initial soil moisture. *Soil Science Society of America Journal*, 19(1), 1–6. Available from: <https://doi.org/10.2136/sssaj1955.03615995001900010001x>
- Bouyoucos, G.J. (1962) Hydrometer method improved for making particle size analysis of soils¹. *Agronomy Journal*, 54(5), 464–465. Available from: <https://doi.org/10.2134/agronj1962.00021962005400050028x>
- Brooks, R.H. & Corey, A.T. (1964). Hydraulic properties of porous media. *Hydrology Papers*. Colorado State University, Fort Collins. No. 3: 37 p.
- Chari, M.M., Poozan, M.T. & Afrasiab, P. (2020) Modelling soil water infiltration variability using scaling. *Biosystems Engineering*, 196, 56–66. Available from: <https://doi.org/10.1016/j.biosystemseng.2020.05.014>
- Cheng, Q., Tang, C.S., Xu, D., Zeng, H. & Shi, B. (2021) Water infiltration in a cracked soil considering effect of drying-wetting cycles. *Journal of Hydrology*, 593, 125640. Available from: <https://doi.org/10.1016/j.jhydrol.2020.125640>
- Clemmens, A.J. (1983). Infiltration equations for border irrigation models. In: *Advances in infiltration*. Proc. Nat. Conf. on Advances in Infiltration. Dec. 12–13. Chicago, Ill. ASAE Pub. 11-83. St. Joseph, Mo. 266-274.
- Comegna, V. & Vitale, C. (1993) Space-time analysis of water status in a volcanic Vesuvian soil. *Geoderma*, 60(1–4), 135–158. Available from: [https://doi.org/10.1016/0016-7061\(93\)90023-E](https://doi.org/10.1016/0016-7061(93)90023-E)
- Dagadu, J.S. & Nimbalkar, P.T. (2012) Infiltration studies of different soils under different soil conditions and comparison of infiltration models with field data. *International Journal of Advanced Engineering Technology*, 3(2), 154–157.
- Erie, L.J. (1962) Evaluation of infiltration measurements. *American Society of Agricultural and Biological Engineers*, St. Joseph, Michigan, 5(1), 11–13. Available from: <https://doi.org/10.13031/2013.40922>
- Furman, A., Warrick, A.W., Zerihun, D. & Sanchez, C.A. (2006) Modified Kostiaikov infiltration function: accounting for initial and boundary conditions. *Journal of Irrigation and Drainage Engineering*, 132(6), 587–596. Available from: [https://doi.org/10.1061/\(ASCE\)0733-9437\(2006\)132:6\(587\)](https://doi.org/10.1061/(ASCE)0733-9437(2006)132:6(587))
- Garg, S. & Goel, A. (2019) Infiltration—a critical review. *Sustainable Engineering*, 2018, 111–120. Available from: https://doi.org/10.1007/978-981-13-6717-5_11
- Gee, G.W. & Bauder, J.W. (1986) Particle-size analysis. In: Klute, A. (Ed.) *Method of soil analysis*. Part 1. Physical and mineralogical methods, *Agronomy No.9*, 2nd edition. Madison, WI: American Society of Agronomy.
- Gifford, G.F. (1976) Applicability of some infiltration formulae to rangeland infiltrometer data. *Journal of Hydrology*, 28(1), 1–11. Available from: [https://doi.org/10.1016/0022-1694\(76\)90048-2](https://doi.org/10.1016/0022-1694(76)90048-2)
- Green, W.H. & Ampt, G.A. (1911) Studies of soil physics, part 1. The flow of air and water through soils. *The Journal of Agricultural Science*, 4(1), 1–24. Available from: <https://doi.org/10.1017/S0021859600001441>
- Haghighi, F., Gorji, M., Shorafa, M., Sarmadian, F. & Mohammadi, M.H. (2010) Evaluation of some infiltration models and hydraulic parameters. *Spanish Journal of Agricultural*

- tural Research, 8(1), 210–217. Available from: <https://doi.org/10.5424/sjar/2010081-1160>
- Hajabbasi, M.A. (2006). Evaluation of Kostiaikov, Horton and Philip's infiltration equations as affected by tillage and rotation systems in a clay-loam soil of northwest Iran. In: 18th World Congress of Soil Science. Philadelphia: International Union of Soil Sciences. USA, 13 July. pp. 9-15.
- Harisuseno, D. & Cahya, E.N. (2020) Determination of soil infiltration rate equation based on soil properties using multiple linear regression. *Journal of Water and Land Development*, 47, 77–88. Available from: <https://doi.org/10.24425/jwld.2020.135034>
- He, Y., Hu, K.L., Wang, H., Huang, Y.F., Chen, D.L., Li, B.G. et al. (2013) Modeling of water and nitrogen utilization of layered soil profiles under a wheat–maize cropping system. *Mathematical and Computer Modelling*, 58(3–4), 596–605. Available from: <https://doi.org/10.1016/j.mcm.2011.10.060>
- Hillel, D. (1998) *Environmental soil physics*. San Diego, CA: Academic Press.
- Horn, R.V. (1993) *Statistical indicators: for the economic and social sciences*. NY: Cambridge University Press 227 pp. [10.1017/CBO9780511518164](https://doi.org/10.1017/CBO9780511518164).
- Horton, R.E. (1940) An approach towards the physical interpretation of infiltration-capacity. *Soil Science Society of America Proceedings*, 5(C), 399–417. Available from: <https://doi.org/10.2136/sssaj1941.036159950005000C0075x>
- Hsu, S.Y., Huang, V., Park, S.W. & Hilpert, M. (2017) Water infiltration into prewetted porous media: dynamic capillary pressure and Green-Ampt modeling. *Advances in Water Resources*, 106, 60–67. Available from: <https://doi.org/10.1016/j.advwatres.2017.02.017>
- Jha, M.K., Mahapatra, S., Mohan, C. & Pohshna, C. (2019) Infiltration characteristics of lateritic vadose zones: field experiments and modeling. *Soil and Tillage Research*, 187, 219–234. Available from: <https://doi.org/10.1016/j.still.2018.12.007>
- Kostiakov, A.N. (1932). On the dynamics of the coefficient of water percolation in soils and on the necessity for studying it from a dynamic point of view for purposes of amelioration. In: *Proc. Transactions of the 6th Communication of the International. Soil Science, Russian Part A, Moscow*, pp. 17-21.
- Liu, J., Zhang, J. & Feng, J. (2008) Green–Ampt model for layered soils with nonuniform initial water content under unsteady infiltration. *Soil Science Society of America Journal*, 72(4), 1041–1047. Available from: <https://doi.org/10.2136/sssaj2007.0119>
- Ma, W., Zhang, X., Zhen, Q. & Zhang, Y. (2016) Effect of soil texture on water infiltration in semiarid reclaimed land. *Water Quality Research Journal of Canada*, 51(1), 33–41. Available from: <https://doi.org/10.2166/wqrjc.2015.025>
- Ma, Y., Feng, S., Su, D., Gao, G. & Huo, Z. (2010) Modeling water infiltration in a large layered soil column with a modified Green–Ampt model and HYDRUS-1D. *Computers and Electronics in Agriculture*, 71, S40–S47. Available from: <https://doi.org/10.1016/j.compag.2009.07.006>
- Ma, Y., Feng, S., Zhan, H., Xiaodong Liu, M.S., Dongyuan Su, M.S., Kang, S. et al. (2011) Water infiltration in layered soils with air entrapment: modified Green-Ampt model and experimental validation. *Journal of Hydrologic Engineering*, 16(8), 628–638. Available from: [https://doi.org/10.1061/\(ASCE\)HE.1943-5584.0000360](https://doi.org/10.1061/(ASCE)HE.1943-5584.0000360)

- Machiwal, D., Jha, M.K. & Mal, B.C. (2006) Modelling infiltration and quantifying spatial soil variability in a wasteland of Kharagpur, India. *Biosystems Engineering*, 95(4), 569–582. Available from: <https://doi.org/10.1016/j.biosystemseng.2006.08.007>
- Mao, L., Li, Y., Hao, W., Zhou, X., Xu, C. & Lei, T. (2016) A new method to estimate soil water infiltration based on a modified Green–Ampt model. *Soil and Tillage Research*, 161, 31–37. Available from: <https://doi.org/10.1016/j.still.2016.03.003>
- Mezencev, V.J. (1948) Theory of formation of the surface runoff. *Meteorologiae Hidrologia*, 3, 33–40.
- Mishra, S.K., Tyagi, J.V. & Singh, V.P. (2003) Comparison of infiltration models. *Hydrological Processes*, 17(13), 2629–2652. Available from: <https://doi.org/10.1002/hyp.1257>
- Mohammadzadeh-Habili, J. & Heidarpour, M. (2015) Application of the Green–Ampt model for infiltration into layered soils. *Journal of Hydrology*, 527, 824–832. Available from: <https://doi.org/10.1016/j.jhydrol.2015.05.052>
- Moore, I.D. & Eigel, J.D. (1981) Infiltration into two layered soil profiles. *Transactions of ASAE*, 24(6), 1496–1503. Available from: <https://doi.org/10.13031/2013.34480>
- Nash, J.E. & Sutcliffe, J.V. (1970) River flow forecasting through conceptual models part I—a discussion of principles. *Journal of Hydrology*, 10(3), 282–290. Available from: [https://doi.org/10.1016/0022-1694\(70\)90255-6](https://doi.org/10.1016/0022-1694(70)90255-6)
- Navar, J. & Synnott, T.J. (2000) Soil infiltration and land use in Linares, NL, Mexico. *Terra Latinoamericana*, 18(3), 255–262.
- Nielsen, D.R., Biggar, J.W. & Erh, K.T. (1973) Spatial variability of field-measured soil-water properties. *Hilgardia*, 42(7), 215–259. Available from: <https://doi.org/10.3733/hilg.v42n07p215>
- Oku, E. & Aiyelari, A. (2011) Predictability of Philip and Kostiakov infiltration models under inceptisols in the humid forest zone, Nigeria. *Agriculture and Natural Resources*, 45(4), 594–602.
- Parhi, P.K. (2014) Another look at Kostiakov, modified Kostiakov and revised modified Kostiakov infiltration models in water resources applications. *International Journal of Agricultural Sciences*, 4(3), 138–142.
- Patle, G.T., Sikar, T.T., Rawat, K.S. & Singh, S.K. (2019) Estimation of infiltration rate from soil properties using regression model for cultivated land. *Geology, Ecology, and Landscapes*, 3(1), 1–13. Available from: <https://doi.org/10.1080/24749508.2018.1481633>
- Philip, J.R. (1957) The theory of infiltration: 1. The infiltration equation and its solution. *Soil Science*, 83(5), 345–358. Available from: <https://doi.org/10.1097/00010694-195705000-00002>
- Pirzad, A., Shakiba, M.R., Zehtab-Salmasi, S., Mohammadi, S.A., Sharifi, R.S. & Hassani, A. (2011) Effects of irrigation regime and plant density on essential oil composition of German chamomile (*Matricaria chamomilla*). *Journal of Herbs, Spices & Medicinal Plants*, 17(2), 107–118. Available from: <https://doi.org/10.1080/10496475.2011.584824>
- Schaap, M.G., Leij, F.J. & van Genuchten, M.T. (2001) A computer program for estimating soil hydraulic parameters with hierarchical pedotransfer functions. *Journal of Hydrology*, 251(3–4), 163–176. Available from: [https://doi.org/10.1016/S0022-1694\(01\)00466-8](https://doi.org/10.1016/S0022-1694(01)00466-8)

- Sihag, P., Tiwari, N.K. & Ranjan, S. (2017) Estimation and inter-comparison of infiltration models. *Water Science*, 31(1), 34–43. Available from: <https://doi.org/10.1016/j.wsj.2017.03.001>
- Šimůnek, J., Köhne, J.M., Kodesová, R. & Šejna, M. (2008) Simulating nonequilibrium movement of water, solutes, and particles using HYDRUS: a review of recent applications. *Soil and Water Research*, 3(Special Issue 1), 42–51.
- Simunek, J., Šejna, M., Saito, H., Sakai, M. & van Genuchten, M.T. (2005) The HYDRUS-1D software package for simulating the one-dimensional movement of water, heat, and multiple solutes in variably-saturated media. *University of California-Riverside Research Reports* 3, 1–240.
- Soil Survey Staff. (2004). *Soil survey laboratory methods manual*. Version No. 4.0. USDA-NRCS. Soil Survey Investigations Report No. 42. U.S. Govt. Print. Office, Washington, DC.
- Turner, E.R. (2006). Comparison of infiltration equation and their field validation by rainfall simulation. Msc. Thesis, Dept. of Biological Resources Engineering, University of Maryland, USA, p. 95.
- van Genuchten, M.T. (1980) A closed-form equation for predicting the hydraulic conductivity of unsaturated soils. *Soil Science Society of America Journal*, 44(5), 892–898. Available from: <https://doi.org/10.2136/sssaj1980.03615995004400050002x>
- van Genuchten, M.V., Leij, F.J. & Yates, S.R. (1991). *The RETC code for quantifying the hydraulic functions of unsaturated soils*. Riverside, CA: Environmental Research Laboratory, US Environmental Protection Agency.
- Wang, Q., Shao, M. & Horton, R. (1999) Modified Green and Ampt models for layered soil infiltration and muddy water infiltration. *Soil Science*, 164(7), 445–453. Available from: <https://doi.org/10.1097/00010694-199907000-00001>